Journal of Visualization, Vol. 7, No. 2 (2004) 135-142

Interaction of Two Parallel Plane Jets of Different Velocities

Fujisawa, N.*[1], Nakamura, K.*[1] and Srinivas, K.*[2]

*1 Department of Mechanical and Production Engineering, Niigata University, 8050 Ikarashi 2, Niigata, 950-2181, Japan.
*2 School of Aerospace, Mechanical and Mechatronic Engineering, University of Sydney, NSW 2006, Australia.

Received 18 August 2003
Revised 13 November 2003

Abstract : The interaction of two parallel plane jets of different velocities is studied by flow visualization and PIV measurement to examine the influence of velocity ratio on the development of jets in the initial region. It is found that the parallel plane jets develop toward the high velocity side and the jet width is reduced with a decrease in the jet velocity ratio. Corresponding to the variation of mean velocity field to the velocity ratio, the magnitudes of turbulence intensities, Reynolds stress and static pressure are weakened in the merging region of the jets and their peak locations of the properties are shifted to the high velocity side. These results indicate that the interaction of two parallel jets is weakened with a decrease in the velocity ratio of the jets.

Keywords : Parallel jets, Flow measurement, Turbulent flow, PIV, Flow visualization

1. Introduction

Interaction of two parallel jets from closely placed nozzles has been studied to understand the fundamental physics of fluids in industrial problems, such as the gas turbine combustion chamber, the air conditioner unit for automobile, the air curtain unit for refrigerator system and so on. These are very important problems in industrial fluid dynamics.

The flow pattern of the two parallel plane jets is shown in Fig. 1. In general, the flow field can be classified into three parts: the conversing region, where the reverse flow is created near the nozzle exit; the merging region, where the velocity profile shows two local peaks without reverse flow; the combined region, where the velocity profile becomes similar to that of the single free jet.

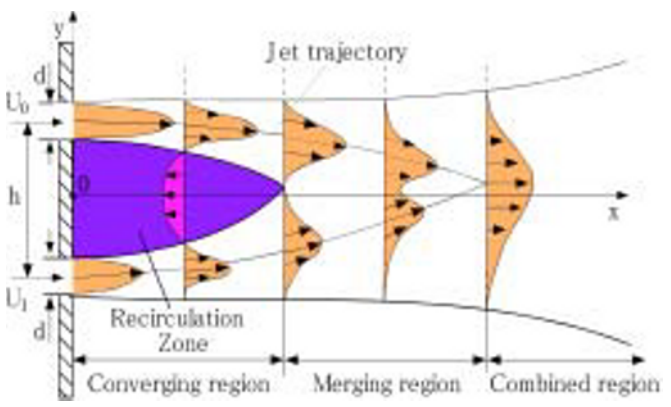

Fig. 1. Schematic illustration of two parallel plane jets.

The essential feature of the flow is the entrainment of the surrounding fluid by turbulent jets, which causes a sub-atmospheric pressure region between the jets near the nozzles. The jets draw each other and their trajectories deviate

from straight lines because of mutual entrainment of the surrounding fluid. The fundamental characteristics of two parallel plane jets have been studied by Miller and Comings(1960), Tanaka(1974), Murai et al.(1976), Ko and Lau(1989), Lin and Sheu(1991), Nasr and Lai(1997a, 1997b) and others. Most of these are concerned with the initial region, where the flow field of the two parallel jets is quite different from that of the single jets due to the interaction of two jets. They measured the cross-sectional distribution of mean flow and turbulence characteristics of the two parallel plane jets by using hot-wire anemometry and laser Doppler velocimetry. The experiments cover a wide range of flow parameters, such as the nozzle separation distances from 2.5 to 40 times the nozzle width and the Reynolds number from 3,000 to 60,000, but they are limited to the parallel plane jets of the same velocities. The development of two parallel jets of different velocities has not been studied in the previous works in spite of its fundamental importance.

The purpose of the present paper is to study the flow characteristics of the two parallel plane jets of different velocities issuing into a quiescent environment. The flow field is visualized by dye injection method and the mean-flow and turbulence properties of the two parallel jets are measured by particle image velocimetry (PIV) to examine the influence of velocity ratio on the development of the two parallel plane jets. The static pressure contour is also obtained in the present study, which is estimated by the Poisson equation for pressure and the mean velocity data from PIV.

2. Experimental Apparatus and Procedure

2.1 Experimental Apparatus

The experiments are carried out in water tank in Fig. 2. The water is driven by two pump units to generate the two parallel plane jets of different velocities. The water goes into two conduits at the bottom of the test tank and returns to the top of the tank. The dimension of the tank is 300mm in height, 400mm in width and 150mm in depth. The width of each nozzle is d=4mm, so that the aspect ratio of each nozzle is 37.5. The separation distance between the nozzle centerlines is set to 3 times the nozzle width (=3d). The size of the test section was determined not to disturb the jet flows, which was examined by the numerical simulation, based on the k-ε model of turbulence.

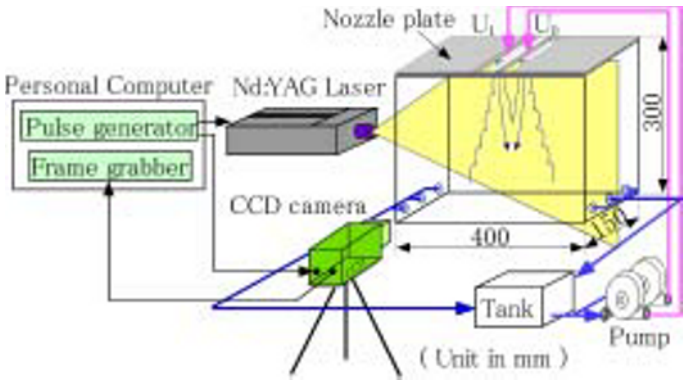

Fig. 2. Experimental apparatus and measurement system.

The velocity U_0 at the reference nozzle exit was kept at 0.3m/s in the present experiment, so that the Reynolds number Re(=$U_0 d/\nu$) was 1,200, where U_0 is the jet velocity at the nozzle exit and d is the nozzle height and ν is the viscosity of the fluid. The velocity U_1 at the other nozzle exit was varied in the range from 0.3m/s to 0.075m/s, which corresponds to the velocity ratio Vr(=U_1/U_0)=1 to 0.25.

2.2 Visualization of Flow Field

The interaction of two parallel plane jets of different velocities is visualized by injecting a dilute solution of Rhodamine B and Fluorescein. When the illumination was provided by a laser sheet of Ar laser, the color of the solution appears orange for the Rhodamine B and green for the Fluorescein. The thickness of the laser sheet was set to 3mm. It is to be noted that these dyes are injected upstream of the nozzles and the high-velocity jet is visualized by the Rhodamine B and the other jet

by the Fluorescein. The visualized images were recorded by a color CCD camera at the frame rate 125frames/s with the shutter speed 1/1000s.

2.3 PIV Measurement of Flow Field

The mean and turbulence properties are measured by particle image velocimetry (PIV), which consists of double pulsed Nd:YAG lasers, pulse generator, digital CCD camera and frame grabber. The schematic illustration of the PIV system is shown in Fig. 2. The visualization of the flow field was carried out by tracer method using nylon tracer particles of 20 μ m in diameter with a specific gravity 1.02. The flow field is illuminated by a Nd:YAG laser-light-sheet having 1mm thickness, and the visualized flow images are taken by the digital CCD camera, which has a spatial resolution of 1018×1008 with 8 bits in gray level. The camera was operated in a double exposure mode and synchronized with the pulse signal from a pulse generator installed in a personal computer, which also controlled the instant of the laser illumination. The wavelength of the Nd:YAG laser is 532nm and the pulse energy is set to 20mJ. The time interval between the successive laser-pulses is set to 80 μ s. The target image has an actual area of 35mm×35mm, so that the spatial resolution of the image is about 35 μ m/pixel. The tracer particle was observed to be about 2 pixels in the image.

The instantaneous velocity distributions were analyzed by using a gray-level difference method for the cross-correlation calculation between the two successive images. The sizes of interrogation window and search window were set to 31×31 pixels and 51×51 pixels, respectively, of which the combination was found to minimize the error vectors with enough spatial resolution. The sub-pixel interpolation process with Gaussian-peak-fitting technique was incorporated into the analysis to improve the accuracy of the velocity measurement. The uncertainty interval of the velocity measurement at 95% coverage was found to be 3%. The statistical properties of the flow field were evaluated from 300 instantaneous velocity distributions. For further details see Tomimatsu and Fujisawa (2002).

2.4 Evaluation of Static Pressure Distribution

The static-pressure distribution of the flow is evaluated from the turbulent Poisson equation for pressure, which is derived from the incompressible Navier-Stokes equations by applying the divergence operation (Gurka et al.,1999). Dirichlet boundary conditions were set at the inlet, while the Neumann condition was prescribed at the other boundaries.

The turbulent Poisson equation for pressure was solved using the two-dimensional mean and turbulence data obtained by PIV measurement. It is to be noted that the turbulent Poisson equation was discretised using the finite differences for pressure, and the pressure gradients were expressed in terms of the mean velocity using the Navier-Stokes equation. Then, the finite difference equation was solved by SOR scheme using the experimental mean velocity data. Further details of the computation are described by Fujisawa and Sato(2001), which also provides the experimental validation of this evaluation method for pressure using a combustion chamber model.

3. Results and Discussion

3.1 Flow Visualization

Figures 3(a) and (b) show the flow visualization images of the two parallel plane jets of different velocities. When the velocities at the exits of the two nozzles are equal (Fig. 3(a)), the two jets merge downstream and the jet trajectory is symmetrical about the centerline. A recirculating region is found between the two jets near the nozzles and they merge downstream of the recirculating region, which is followed by the intense turbulent mixing of the two jets. On the other hand, the flow field is modified by the influence of different velocities, as shown with Fig. 3(b), where the velocity ratio

Vr(=U_1/U_0) is 0.5. The low-velocity jet is directed to the high velocity side and the combined jets develop inclining to the high velocity side. Therefore, the trajectory of the two parallel plane jets is modified by the influence of jet velocity ratio, which indicates a different entrainment rate for each jet. The entrainment rate is larger on the high-velocity jet, because it is proportional to the jet velocity. It is noted that the turbulent mixing between the parallel jets is weakened and the jet width is narrowed with a decrease in the velocity ratio, which is reflected by the smaller entrainment rate on the low-velocity jet and the corresponding smaller momentum of the jet.

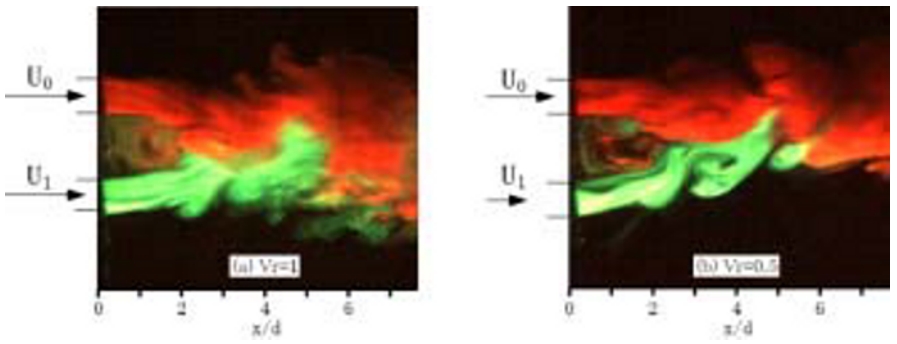

Fig. 3. Visualization of two parallel plane jets.

3.2 Mean-flow Characteristics

Typical examples of the velocity vectors and the velocity magnitudes of two parallel plane jets are shown in Figs. 4(a), (b), (c) and (d) for Vr=1, 0.75, 0.5 and 0.25, respectively. The two jets merge

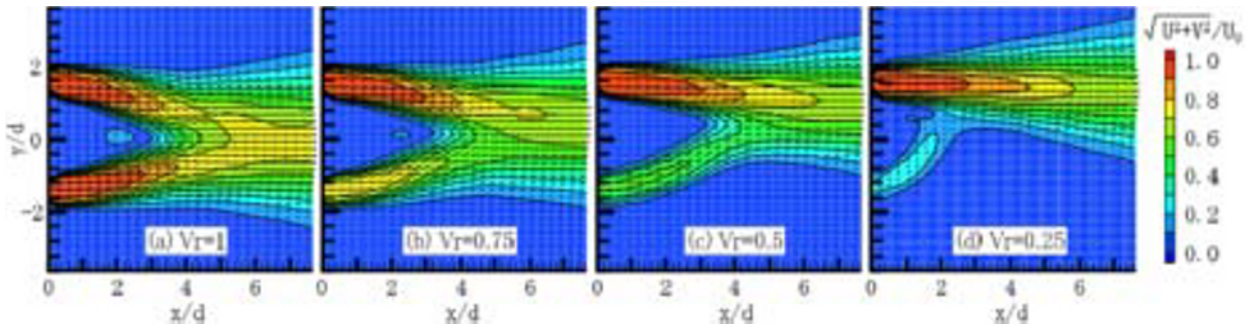

Fig. 4. Mean velocity vectors and contour of velocity magnitude.

around x/d=3 and the jet trajectories combine around x/d=6, which agree with the observations by Ko and Lau (1989), in spite of the different nozzle distances and Reynolds numbers. When the jet velocity ratio is reduced to Vr=0.75, the inclination angle of the high-velocity jet is reduced and it develops more horizontally downstream than that of Vr=1. It is expected that this modification of jet trajectory is caused by the smaller entrainment on the low-velocity jet. With further decrease in jet velocity at Vr=0.5, the reduction in the jet width is clearly observed in the flow field. When the jet velocity U_1 is further decreased to Vr=0.25, the combined jets develop almost horizontally like a single free jet. The low-velocity jet is dragged into the high-velocity jet immediately after issuing from the nozzle, so that the merging distance becomes shorter at Vr=0.25. The recirculating region downstream of the nozzle shifts to the high-velocity side with a decrease in the velocity ratio, which coincides with the visual observation in Fig. 3. Therefore, the flow field induced by the two parallel plane jets of different velocities becomes asymmetric about the jet centerline.

Figure 5 shows the variations of the jet width (Fig. 5(a)), the maximum velocity (Fig. 5(b)) and the position of maximum velocity (Fig. 5(c)) at various velocity ratios Vr=1, 0.75, 0.5, 0.25. The jet width b in Fig. 5(a) is defined as the distance between outer-half-width positions of each jet having a

peak in the velocity distribution, and it turns out to be the usual definition of half width of jet having a single peak in the velocity distribution. Therefore, the measured jet width b has a gap at the merging point of the two parallel jets, where the velocity distribution changes from two peaks to a single peak. With an increase in the streamwise distance from the nozzle, the jet width of the two parallel jets of the same velocities decreases gradually and reaches a minimum around the point x/d=4-6 and it increases further downstream. The variation of jet width agrees with the observation by Ko and Lau(1989). When the velocity ratio of the two parallel jets is decreased, the jet width is narrower than that for Vr=1, which is apparently observed around the merging point.

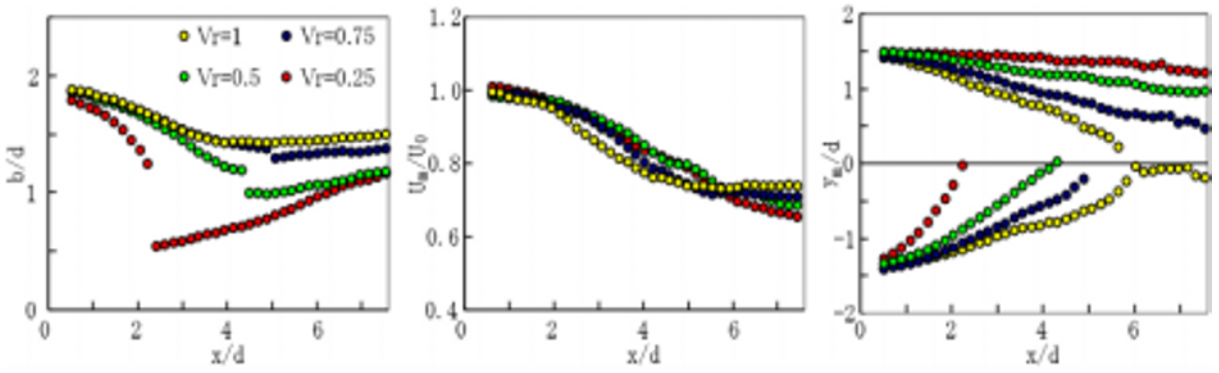

(a)Jet width (b) Maximum velocity (c) Position of maximum velocity

Fig. 5. Downstream variations and mean flow characteristics of parallel plane jets.

The decay of the maximum velocity in Fig. 5(b) shows less influence of jet velocity ratio on the maximum velocity, compared with that of the jet width in Fig. 5(a). However, the detail examination shows an increase in maximum velocity in the range x/d=2-5.5 and a decrease in the range x/d>5.5, when the jet velocity ratio is decreased. It is to be mentioned that the variation of the maximum velocity does not correspond to that of the jet width, which is due to the definition of the jet width.

The position of the maximum velocity of the two parallel plane jets is shown in Fig.5(c). When the jet velocity ratio is Vr=1, two jets combine around x/d=6 and the maximum velocity is on the jet centerline further downstream. With a decrease in the jet velocity ratio, the combined point moves upstream and the trajectory of maximum velocity shifts to the high velocity side. Therefore, the trajectory of the two parallel plane jets is greatly influenced by the variation in velocity ratio.

3.3 Turbulence Characteristics

Figures 6 and 7 show the contours of streamwise and normal turbulence intensities, respectively. The contour of streamwise turbulence intensity of the two parallel jets of the same velocities shows a high peak along both sides of the jet shear-layer up to x/d=3-4, while low turbulence intensity is observed in the potential core region of the two parallel jets. Further downstream at x/d=4-6, the high peaks of streamwise turbulence intensity gather to the jet centerline and their magnitudes are weakened.

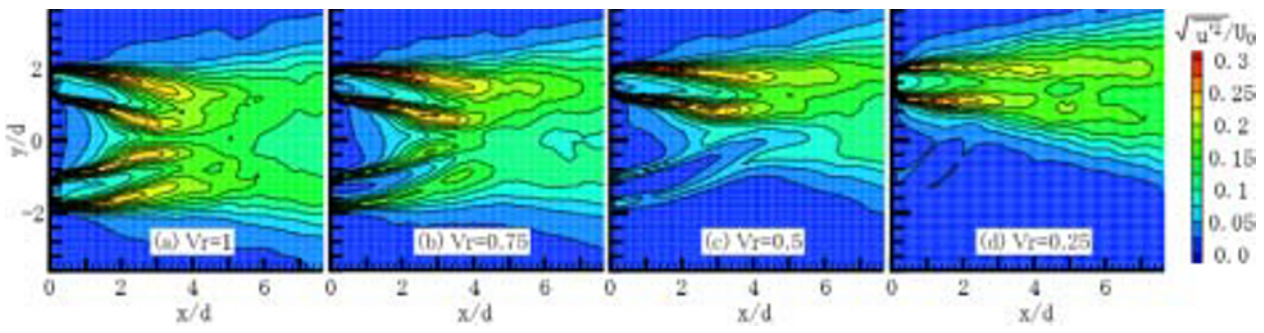

Fig. 6. Contour of streamwise turbulence intensity.

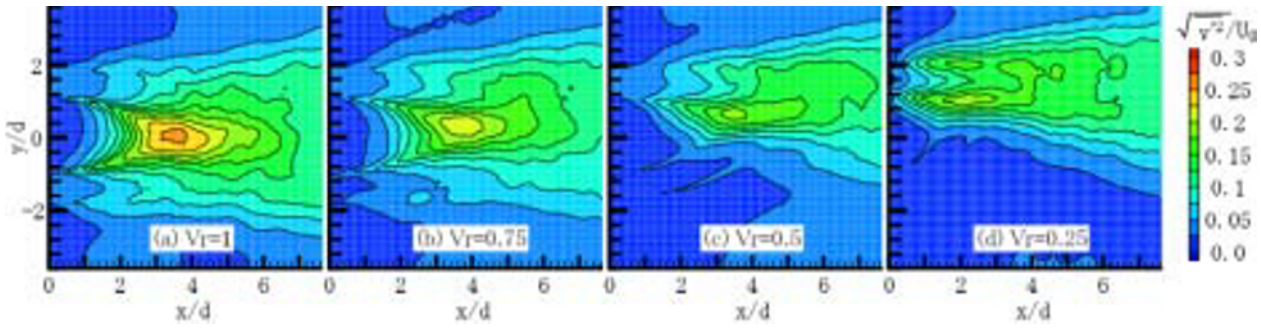

Fig. 7. Contour of normal turbulence intensity.

It is noted that the streamwise turbulence intensity in the jet centerline is slightly smaller than that of the outer area for x/d>6, which indicates the feature of turbulence in free jets as reported by Eberitt and Robins(1978). On the other hand, the normal turbulence intensity for Vr=1 (Fig.7(a)) shows a gradual increase along the jet shear layer to the downstream near the nozzle exit, which is followed by the high peak at x/d=3-4. Then, it gradually decreases with an increase in the streamwise distance. Note that the maximum is on the jet centerline. Therefore, the contour of the turbulence intensities in the two parallel plane jets shows an intense interaction between the jets in the merging region and approaches that of the single free jet in the downstream.

With a decrease in the jet velocity ratio Vr, the streamwise and normal turbulence intensities decrease on the low velocity side and the width of the turbulent region becomes narrower than that of Vr=1. These variations of turbulence intensities are consistent with the variation of jet trajectories in Fig. 5(c). Such changes in turbulence intensity contours are caused by the smaller mean velocity on the low-velocity jet, which results in the reduced interaction of two jets with a decrease in the velocity ratio.

Figure 8 shows the contour of Reynolds stress for various velocity ratios. The contours for the same velocities show a high peak along the inner shear layer especially at the merging region x/d=3-4, while the low peaks are created along the outer shear layer of the jets. This indicates the strong interaction of the two jets at the merging region. The sign of the Reynolds stress is positive on the upper outer-shear-layer and lower inner-shear-layer, and is negative in the upper inner-shear-layer and the lower outer-shear-layer. These are reflected by the velocity gradients of each jet. Further downstream, high peaks in the inner shear layer are reduced and the low peaks in the outer shear layer are promoted. This results in small peaks at off-center positions in the cross-sectional distribution as observed in a fully developed free jet by Eberitt and Robins(1978).

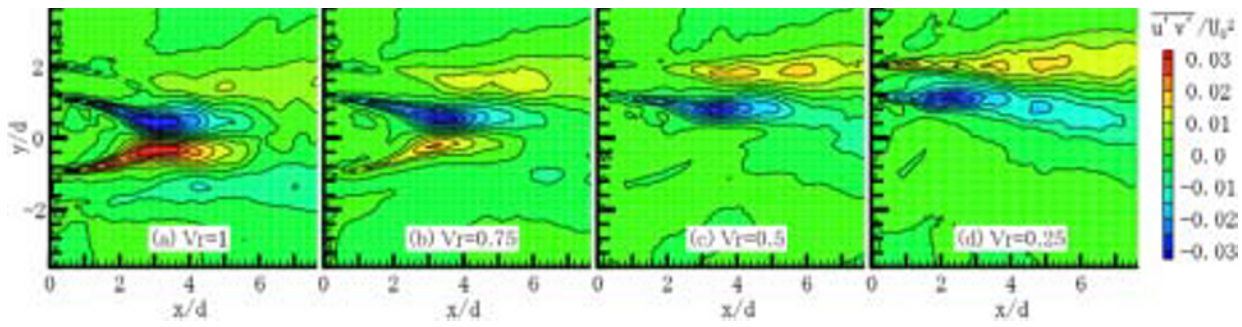

Fig. 8. Contour of Reynolds stress.

When the velocity ratio Vr is decreased, the magnitude of the Reynolds stress in the inner shear-layer is reduced and that in the outer shear-layer is increased. Therefore, the Reynolds stress contour approaches that of the single free jet with a decrease in the velocity ratio. The reduction of the Reynolds stress magnitude in the inner shear-layer is caused by the reduction of the velocity

gradient between the two jets, while the recovery of the Reynolds stress in the outer shear-layer is due to the reduced influence of the streamline curvature in the converging and merging region of the two jets (Kobayashi and Fujisawa 1983).

3.4 Static Pressure Contour

The static pressure plays a significant role in the flow characteristics of the two parallel plane jets. Therefore, the contour of static pressure is evaluated from the turbulent Poisson equation using the measured mean velocity data by PIV.

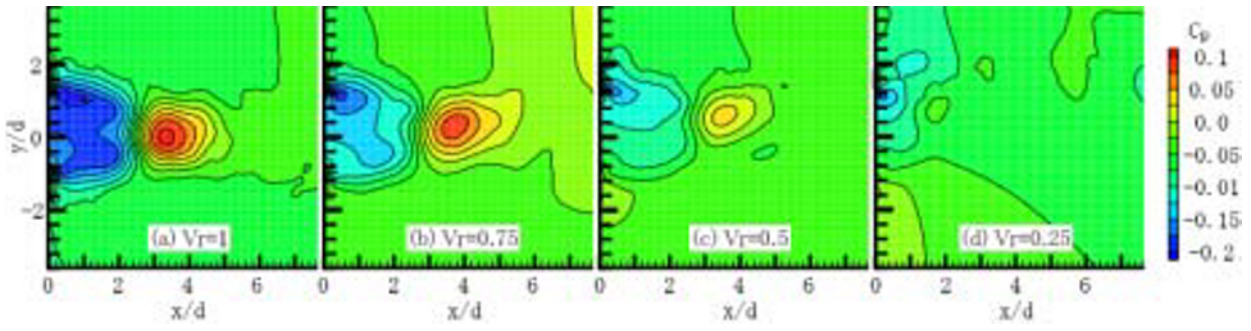

Fig. 9. Contour of static pressure.

Figure 9 shows the contour of static pressure in the parallel plane jets at various velocity ratios. The static pressure coefficient C_p is defined by $C_p=2(p-p_0)/\rho U_0^2$, where p is the static pressure, p_0 is the reference static pressure at nozzle exit of high-velocity jet and ρ is the density of fluid. The static pressure contour for Vr=1 shows a low pressure region in the recirculating region and a high pressure region in the merging region, which is followed by the recovery of pressure in the downstream. The present result agrees qualitatively with the measurement using the static pressure tube (Miller et al. 1960, Murai et al. 1976, Nasr and Lai 1997a).

When the velocity ratio is decreased, the magnitude of the static pressure in the two parallel jets is reduced and the position of pressure peak is shifted to the high-velocity side, which is consistent with the variation of mean velocity field (Fig. 4), jet trajectory (Fig. 5(c)), and turbulence characteristics (Fig. 6-8). The reduction of static pressure in the two parallel jets at lower velocity ratios indicates the reduced interaction of the two jets, which is due to the smaller entrainment rate and the corresponding smaller momentum of the low-velocity jet. Therefore, the present result indicates that the attraction of the two jets is weakened with a decrease in the velocity ratio.

4. Conclusion

The interaction of two parallel plane jets of different velocities is studied by flow visualization and PIV measurement to examine the influence of velocity ratios on the mean and turbulence characteristics of the jets in the initial region. When the velocity ratio is decreased, the jet trajectory of the two parallel plane jets moves to the high velocity side and the width of the jet is reduced. Therefore, the two parallel plane jets approach the single free jet with a decrease in the velocity ratio. Corresponding to the variation of the mean flow characteristics, the turbulence intensities and the Reynolds stress are reduced in the merging region of the jet with a decrease in the velocity ratio. The variation of static pressure contour in the parallel jets is examined using the turbulent Poisson equation for pressure with the mean velocity data from PIV. It is found that the variation of the static pressure in the merging region is reduced and the peak position is shifted to the high velocity side with a decrease in the velocity ratio. These results indicate that the interaction of the two parallel jets is weakened and the flow characteristics approach that of the single free jet with a decrease in

velocity ratio. The mechanism of jet interaction is due to the entrainment of surrounding fluid near the nozzle exit, which produces the low and high pressure region near the nozzle exit. When the velocity ratio is decreased, the entrainment of the low-velocity jet is reduced and the jet attraction is weakened, which results in a modification of the pressure contour and the jet trajectories in the downstream.

References

Everitt, K. W. and Robins, A. G., The Development and Structure of Turbulent Plane Jets, Journal of Fluid Mechanics, 88 (1978), 563-583.

Fujisawa, N. and Sato, A., Evaluation of Three-dimensional Flow and Pressure Fields in a Cold Model of Combustion Chamber by Plane PIV Measurements, Proc. 4th International Symposium on PIV (Goettingen), (2001), Pa.1072.

Gurka, R., Liberzon, A., Hefetz, D., Rubinstein, D. and Shavit, U., Computation of Pressure Distribution Using PIV Velocity Data, Proc. 3rd International Symposium PIV (Santa Barbara), (1999), 671-676.

Ko, N. W. M. and Lau, K. K., Flow Structures in Initial Region of Two Interacting Parallel Plane Jets, Experimental Thermal and Fluid Science, 2 (1989), 431-449.

Kobayashi, R. and Fujisawa, N., Curvature Effects on Two-dimensional Turbulent Wall Jets, Ingenieur Archiv, 53 (1983), 409-417.

Lin, Y. F. and Sheu, M. J., Interaction of Two Plane Parallel Unventilated Jets, Experiments in Fluids, 10 (1990), 17-22.

Miller, D. R. and Comings, E. W., Force-momentum Fields in a Dual-jet Flow, Journal of Fluid Mechanics, 7 (1960), 237-256.

Murai, K., Taga, M. and Akagawa, K., An Experimental Study on Confluence of Two Two-dimensional Jets, Bulletin of JSME, 19 (1976), 958-964.

Nasr, A. and Lai, J. C. S., Two Parallel Plane Jets: Mean Flow and Effects of Acoustic Excitation, Experiments in Fluids, 22 (1997a), 251-260.

Nasr, A. and Lai, J. C. S., Comparison of Flow Characteristics in the Near Field of Two Parallel Plane Jets and an Offset Plane Jet, Physics of Fluids, 9 (1997b), 2919-2931.

Tanaka, E., The Interference of Two-dimensional Parallel Jets: Experiments on Dual Jet, Bulletin of JSME, 13 (1970), 272-280.

Tomimatsu, S., Fujisawa, N. and Hosokawa, A., PIV Measurement of Velocity Field in Spray Combustor, Journal Visualization, 6 (2003), 273-281.

Author Profile

Nobuyuki Fujisawa: After graduating from Tohoku University (D.E. 1983), he joined Gunma University in 1983 and worked as an associate professor since 1991. He has been a professor of Niigata University since 1997 and is continuing research on the visualization and non-intrusive measurement of velocity, temperature and shear stress in mechanical engineering.

Koichi Nakamura: He was educated at Niigata University (B.E. 2001). He is now studying at Graduate School of Niigata University and continuing research on interaction of jets.

Srinivas Karkenahalli: He is a Senior Lecturer at the School of Aerospace, Mechanical and Mechatronic Engineering, University of Sydney, Australia. His interests are optimization of aerodynamic shapes using evolutionary algorithms and computational fluid dynamics.